On the zeros of the q-analogue exponential function

1994 J. Phys. A: Math. Gen. 27 3857

(http://iopscience.iop.org/0305-4470/27/11/034)

J. Phys. A: Math. Gen. 27 (1994) 3857–3881. Printed in the UK

On the zeros of the q-analogue exponential function

Charles A Nelson and Michael G Gartley

Department of Physics, State University of New York at Binghamton, Binghamton, NY 13902-6000, USA

Received 12 July 1993, in final form 14 December 1993

Abstract. An asymptotic formula for the zeros, z_n, of the entire function $e_q(x)$ for $q \ll 1$ is obtained. As q increases above the first collision point at $q_1^* \approx 0.14$, these zeros collide in pairs and then move off into the complex z plane. They move off as (and remain) a complex conjugate pair. The zeros of the ordinary higher derivatives and of the ordinary indefinite integrals of $e_q(x)$ vary with q in a similar manner. Properties of $e_q(z)$ for z complex and for arbitrary q are deduced. For $0 \leqslant q < 1$, $e_q(z)$ is an entire function of order 0. By the Hadamard–Weierstrass factorization theorem, infinite product representations are obtained for $e_q(z)$ and for the reciprocal function $e_q^{-1}(z)$. If $q \neq 1$, the zeros satisfy the sum rule $\Sigma_{n=1}^{\infty} (1/z_n) = -1$.

1. Motivation

The q-exponential function [1, 2], which occurs [3, 4] in the study of quantum algebras, is defined by

$$e_q(z) \equiv \sum_{n=0}^{\infty} \frac{z^n}{[n]!} \tag{1}$$

where $[n]! = [n]\,[n-1] \ldots [1]$, $[0]! = 1$. The 'bracket #' for q real and positive is defined by

$$[x]_q = [x] = \frac{q^{x/2} - q^{-x/2}}{q^{1/2} - q^{-1/2}} \tag{2}$$

and is called the 'q-deformation' of x. It, and $e_q(z)$, are invariant under $q \leftrightarrow 1/q$. So, unless noted otherwise, we take $0 < q < 1$ in this paper.

As $q \to 1$, $e_q(z) \to \exp(z)$ and as $q \to 0$, $e_q(z) \to 1 + z$. From (1), we see that $e_q(z)$ is an entire function (a transcendental entire function) and $|e_q(z)| \leqslant e_q(|z|) \leqslant \exp(|z|)$. So the series representation converges uniformly and absolutely for all finite z independent of the value of q. $e_q(z)$ has an essential singularity at infinity. For $x > 0$, $e_q(x)$ is positive. But for $x < 0$, we have an alternating series. For $x < 0$ and $q < \sim 0.14$ there is a universal

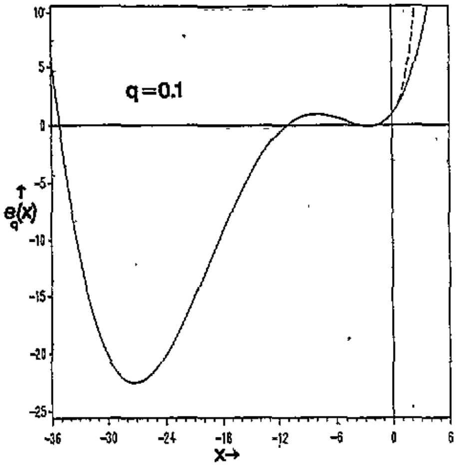

Figure 1. Plot showing universal behaviour of $e_q(x)$ for $q<q_1^*$ ($q_1^*\approx 0.14$). The broken curve for x positive is $\exp(x)$.

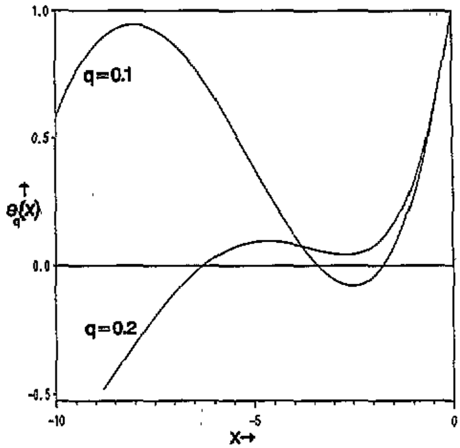

Figure 2. An enlargement of the preceding figure, $e_q(x)$ for $q=0.1$, in the small negative x region. The curve for $q=0.2$ shows the dip that occurs in $e_q(x)>0$ after a collision of an associated-pair of zeros. At $q_1^*\approx 0.14$ the first two zeros, z_1 and z_2, collide and move off the negative real axis into the complex z-plane. They move off as (and remain) a complex conjugate pair.

behaviour independent of the value of q consisting of increasing amplitude oscillations of decreasing frequency as $x\to(-\infty)$ (see figures 1 and 2).

However, not much is known quantitatively about $e_q(z)$. In particular, little is known about its zeros. These zeros and the properties of $e_q(x)$ for x negative appear prominently in a completeness relation [5, 9] for the q-analogue coherent states (CS)

$$\int |z\rangle_{q\,q}\langle z|\,\mathrm{d}\mu(z)+\int|\tilde{z}\rangle_{q\,q}\langle\tilde{z}|\,\mathrm{d}\tilde{\mu}=1. \tag{3}$$

Thus, in quantum field theory the properties of $e_q(z)$ are also important for the various q-analogue diagonal operator representations [6, 7] analogous to the P-, Q-, and W-representations in quantum optics.

In (3), the q-analogue CS, $|z\rangle_q$, are eigenstates of the q-boson annihilation operator where z is a complex number, $a|z\rangle_q=z|z\rangle_q$, with

$$aa^+-q^{\pm 1/2}a^+a=q^{\mp N/2} \tag{4}$$

and $[N,a^+]=a^+$, $[N,a]=-a$. Then,

$$|z\rangle_q=N(z)\sum_{n=0}^{\infty}\frac{z^n}{\sqrt{[n]!}}|n\rangle \tag{5}$$

where $N(z)=e_q(|z|^2)^{-1/2}$. For the measure

$$\mathrm{d}\mu(z)=(1/2\pi)e_q(|z|^2)e_q(-|z|^2)\,\mathrm{d}_q|z|^2\,\mathrm{d}\theta \tag{6}$$

the first term in (3) gives [5, 6]

$$\int |z\rangle\langle z|\, \mathrm{d}\mu = \sum_{n=0}^{\infty} \frac{1}{[n]!} \int_0^{\zeta_i} x^n e_q(-x)\, \mathrm{d}_q x |n\rangle\langle n| \tag{7}$$

with $x=|z|^2$. In (7) the integral over $|z|^2$ is a q-integration over the interval from zero to some $\zeta_i>0$ (i fixed) where $-\zeta=-\zeta_1$ is the largest zero of $e_q(z)$, $-\zeta_2$ the next largest, etc.

Note that $e_q(x)$ in the negative x region is the significant factor in the measure. The other factor $e_q(|z|^2)=\{N(z)\}^{-2}$, is required only to cancel the normalization factor of $|z\rangle_q$.

The second term [7] in (3) also depends on the (i fixed) zero ζ_i. The set of *q-discrete* auxiliary states $|\tilde{z}\rangle_q$ are also eigenstates of an $\tilde{a}_k$ annihilation operator (see appendix 2)

$$\tilde{a}_k|\tilde{z}_k\rangle=(q^{1/4}\tilde{z}_k)|\tilde{z}_k\rangle \tag{8}$$

$$|\tilde{z}_k\rangle \equiv M_k \sum_{j=0}^{\infty} \frac{(q^{1/4}\tilde{z}_k)^j}{\sqrt{[j]!}} |j+k\rangle \tag{9}$$

where

$$|\tilde{z}_k|^2 \equiv x_k = q^{k/2}\zeta_i \tag{10}$$

with $k=0, 1, \ldots$; $M_k=e_q(q^{1/2}x_k)^{-1/2}$. So for the discrete measure

$$\mathrm{d}\tilde{\mu}_k=\frac{1}{2\pi M_k^2} e_q(-|\tilde{z}_k|^2)\, \mathrm{d}\theta \tag{11a}$$

$$\int |\tilde{z}\rangle\langle\tilde{z}|\, \mathrm{d}\tilde{\mu} = \sum_{n=0}^{\infty} \sum_{k=0}^{n} \frac{1}{[n-k]!} (q^{1/2}x_k)^{n-k} |n\rangle\langle n| e_q(-x_k). \tag{11b}$$

In (11a) and (11b), e_q in the negative x region also appears. The resolution of unity is satisfied since [5, 7]

$$\int_0^{\zeta_i} e_q(-x)x^n\, \mathrm{d}_q x=[n]!\left\{1-\sum_{k=0}^{n} \frac{(q^{1/2}x_k)^{n-k}}{[n-k]!} e_q(-x_k)\right\} \tag{12}$$

is the q-analogue of Euler's formula for $\Gamma(x)$.

In the completeness relation (3), the separate contributions from the q-bosons and from the auxiliary q-bosons depend on the choice made for the ith zero ζ_i, of $e_q(z)$. It is true that when both terms are combined, this dependence on ζ_i cancels out. Nevertheless, for the q-boson term alone this ζ_i dependence is very important mathematically, by (12), and most likely is also important physically for q values sufficiently different from 1.

Note that the upper integration limit in (12) need not be the absolute value of a zero of e_q. However, for ζ_i as the upper integration limit, the standard Euler identity follows as $q \to 1$.

In complex analysis, the distribution of the zeros of an entire function is connected with the growth of the entire function. This is another reason for a more quantitative study of the zeros of $e_q(z)$.

Lastly, the $e_q(z)$ function frequently appears in the current literature on quantum algebras. Knowledge of the simple properties of e_q, and of the inverse function

$e_q^{-1}(z)$, for z complex and for arbitrary q should be useful to formal investigations, to applications of q-symmetries, and to other applications of the $e_q(z)$ function in physics.

In section 2 we study the properties of the zeros of $e_q(x)$ for $q<q_1^*$ ($q_1^*\approx 0.14$). For $q\ll 1$, asymptotic formulae for these zeros, and for those of its derivatives and indefinite integrals are obtained. Section 3 examines the pairwise collision of associated zeros that is found to occur as q increases above $q_1^*\approx 0.14$. Section 4 then studies the properties of the complex function $e_q(z)$ for z complex and for arbitrary q. In section 5, we show that $e_q(z)$ is an order zero entire function and obtain infinite product representations for $e_q(z)$ and for the reciprocal function $e_q^{-1}(z)$. We show that the zeros of e_q satisfy the sum rule $\Sigma_{n=1}^{\infty}(1/z_n)=-1$ for $q\neq 1$. The properties of Jackson's $E_q(z)$ function are discussed in appendix 1 since it occurs for a simple alternative realization of the q-boson commutation relations. In appendix 2 we briefly review the properties of the auxiliary q-boson operators $\tilde{a}_k$ and $\tilde{a}_k^+$. Appendix 3 contains some additional results about $e_q(z)$.

2. Properties of the zeros of $e_q(x)$ for $q<\sim 0.14$

Since $e_q(x)$ is defined for $x<0$ by a convergent alternating series with terms which monotonically decrease in absolute value (after sufficiently many terms), we can reliably analyse its behaviour numerically since the error in truncating the series is less than the absolute value of the first term dropped, provided the absolute values of the terms have already started to monotonically decrease.

However, before reporting numerical results, we will analytically obtain an asymptotic estimate of the values of the zeros of $e_q(x)$ which is extremely accurate when $q\ll 1$. Exton has shown [1, 2] that a less explicit procedure gives exactly the zeros of Jackson's q-exponential function [10] $E_q(x)$ for $q>1$, and that it gives a good estimate for the zeros of $\cos_q(y)\equiv\mathrm{Re}\{e_q(\mathrm{i}y)\}$ and of $\sin_q(y)\equiv\mathrm{Im}\{e_q(\mathrm{i}y)\}$. The method we propose in this paper gives the same estimates as Exton's in these three instances.

The series representation for the q-exponential function is

$$e_q(z)=\sum_{n=0}^{\infty}\frac{z^n}{[n]!}.$$

When q is small or n large, the deformation of n can be approximated,

$$[n]_q=\frac{q^{(1-n)/2}q^{(1+n)/2}}{1-q}\approx\frac{q^{(1-n)/2}}{1-q} \tag{13a}$$

or

$$[n]_q\approx\frac{p^{2(1-n)}}{1-q} \tag{13b}$$

where

$$p=q^{1/4}\qquad\text{(positive fourth root).} \tag{13c}$$

We use this approximation to estimate $[n]_q!$ and $\log([n]_q!)$ for $n\geqslant 1$:

$$[n]_q!=\frac{p^{-n(n-1)}}{(1-q)^n}\{(1-q)(1-q^2)\ldots(1-q^n)\} \tag{13d}$$

so

$$[0]!\equiv 1$$

and

$$[1]! = \frac{1}{1-q}\{1-q\}$$

$$[2]! = \frac{p^{-2}}{(1-q)^n}\{1-q-q^2+q^3\}$$

$$[n]! = \frac{p^{-n(n-1)}}{(1-q)^n}\{1-q-q^2+\mathrm{O}(q^4)\} \qquad n \geqslant 3 \tag{14a}$$

where the $\mathrm{O}(q^3)$ term vanishes in the last braces for $n \geqslant 3$. Likewise,

$$\log([n]_q!) = -n\{(n-1)\log p + \log(1-q)\} + \log\{(1-q)(1-q^2)\ldots(1-q^n)\}$$

so

$$\log([n]_q!) = -n\{(n-1)\log p + \log(1-q)\} + \log\{1-q-q^2+\mathrm{O}(q^4)\} \qquad n \geqslant 3. \tag{14b}$$

As in applications of Stirling's formulae, for q small or n large we will set the 'brace' equal to '1' in (14a), or set the second 'brace' equal to '1' in (14b), to obtain a simpler 'approximate series' or expression for analytic analysis. For q small (or n large) such an 'approximate series' gives a good estimate of the behaviour of the 'exact series' of interest. When desired, corrections from the brace factors can be systematically included (see appendix 3).

For the q-exponential function, the associated 'approximate series' $e_q^{\mathrm{A}}(x)$ is

$$e_q(x) \to e_q^{\mathrm{A}}(x) \equiv 1 + \sum_{r=1}^{\infty} p^{r^2-r}(1-q)^r x^r. \tag{15}$$

Note that the magnitude of the 'rth term' equals the magnitude of the '$(r-1)$st term' when

$$|x| = \frac{p^{2-2r}}{1-q}.$$

So '$c_r x^r$' is the largest term in magnitude when

$$\frac{p^{2-2r}}{1-q} < |x| < \frac{p^{-2r}}{1-q}.$$

In fact (see appendix 3) at the geometric mean of this interval

$$|\bar{x}| = p\,\frac{p^{-2r}}{1-q}$$

the '$c_r x^r$' term dominates the sum in magnitude for $e_q^{\mathrm{A}}(x)$ when $q < 0.043212\ldots$. Then the sign of $e_q^{\mathrm{A}}(-|\bar{x}|)$ equals $(-)^r$. Thus, $e_q^{\mathrm{A}}(x)$ has infinitely many real negative zeros when $q < 0.043212\ldots$.

So to obtain an asymptotic estimate for the location of the nth zero of $e_q(x)$ we assign x a value $\tilde{\mu}_n^e$ such that the magnitude of the 'nth term' in (15) equals the magnitude of the '$(n-1)$st term'. Thereby, the asymptotic formula for $\tilde{\mu}_n^e$ is

$$\tilde{\mu}_n^e = -\frac{q^{(1-n)/2}}{1-q} \qquad n = 1, 2, \ldots. \tag{16}$$

We denote such asymptotic values by a tilde. For each such asymptotic estimate for the zeros of a specific function which is given in this paper, we numerically find that *for n sufficiently large the associated fractional deviation is monotonic in n, with q fixed* ($q \approx 0.1$ to 0.001).

Actually, for $e_q(x)$ there is a greater cancellation occurring than is suggested by the above reasoning. In fact, for $x = \tilde{\mu}_n^e$ the sum of the '1' plus the first $r_n = 2n-1$ terms in the approximate series $e_q^{\mathrm{A}}(x)$, see (15), vanishes. The remaining terms beyond the r_nth are negligible. In particular, if we use (16) to rescale x_n

$$x_n = \left(\frac{p^{2(1-n)}}{1-q}\right) y_n \tag{17a}$$

then

$$e_q^{\mathrm{A}}(x) = 1 + \sum_{r=1}^{\infty} p^{r(r-2n+1)} y^r. \tag{17b}$$

We call

$$1 + \sum_{m=1}^{2n-1} p^{m(m-2n+1)} y^m = 0 \tag{17c}$$

the 'asymptotic polynomial' for $e_q(x)$. It vanishes for $y_n = -1$ (independent of n), so by (17*a*) the 'improved asymptotic formula' for the zeros of $e_q(x)$ is also (16).

For some of the other functions (*e.g. the derivatives and indefinite integrals of $e_q(x)$*) considered in this paper, 'improved asymptotic values' can be obtained by solving the associated 'asymptotic polynomial' for the q-analogue function of interest. For $y = -1$, the 'asymptotic polynomial' automatically vanishes for the following functions: $e_q(x)$, $\cos_q(y) \equiv \mathrm{Re}\{e_q(\mathrm{i}y)\}$, $\sin_q(y) \equiv \mathrm{Im}\{e_q(\mathrm{i}y)\}$; and for $q > 1$ for $E_q(x)$, $\mathrm{Cos}_q(y)$, and $\mathrm{Sin}_q(y)$, which are discussed in appendix 1.

Table 1 shows that the fractional deviation of $\tilde{\mu}_n$ from the actual real parts, μ_n, is arbitrarily small as $q \to 0$ for the first eight zeros,

$$z_n = \mu_n + \mathrm{i}\nu_n$$

of $e_q(x)$. By (16), $e_q(x)$ has an infinite number of zeros when $q \neq 0$ or 1. By (16), for fixed $q \neq 0$ or 1, the separation between adjacent zeros increases as n increases since

$$\tilde{\mu}_{n+1} - \tilde{\mu}_n = q^{-1/2}(\tilde{\mu}_n - \tilde{\mu}_{n-1}). \tag{18a}$$

So, the frequency of oscillation of $e_q(x)$ decreases as $x \to (-\infty)$. Since

$$\tilde{\mu}_{n+1}/\tilde{\mu}_n = 1/\sqrt{q} \tag{18b}$$

the zeros increase asymptotically in geometric proportion.

Similarly, for the turning points of $e_q(x)$, we find for $n = 1, 2, 3, \ldots$ that

$$\tilde{\tau}_n^e = -\frac{q^{-n/2}}{1-q}\left(\frac{n}{n+1}\right) \tag{19a}$$

Table 1. The fractional deviations, $(\mu_n - \bar{\mu}_n)/\bar{\mu}_n$, of the asymptotic $\bar{\mu}_n$ from the actual real parts μ_n for the first eight zeros. A triple asterisk entry denotes 'fractional deviation' $<10^{-14}$. Horizontal lines show where the collision points occur.

q	$n=1$	$n=2$	$n=3$	$n=4$	$n=5$	$n=6$	$n=7$	$n=8$
0.100	0.362 4	−0.034 97	9.196E−5	−2.901E−8	9.163E−13	***	***	***
0.125	0.434 3	−0.085 77	0.000 3113	−2.143E−7	1.848E−11	***	***	***
0.150	0.524 7	−0.227 1	0.000 8812	−1.149E−6	2.249E−10	***	***	***
0.175	0.511 8	−0.166 9	0.002 208	−4.961E−6	1.942E−9	−1.331E−13	***	***
0.200	0.502 5	−0.112 5	0.005 053	−1.837E−5	1.310E−8	−1.877E−12	***	***
0.225	0.495 3	−0.063 95	0.010 73	−6.081E−5	7.348E−8	−2.007E−11	***	***
0.250	0.489 1	−0.021 76	0.021 21	−0.000 1852	3.583E−7	−1.746E−10	***	***
0.275	0.482 7	0.013 48	0.038 92	−0.000 5312	1.586E−6	−1.289E−9	2.976E−13	***
0.300	0.475 1	0.041 58	0.066 04	−0.001 463	6.310E−6	−8.359E−9	3.366E−12	***
0.325	0.465 8	0.062 98	0.104 0	−0.003 951	2.380E−5	−4.887E−8	3.273E−11	***
0.350	0.454 9	0.078 57	0.154 3	−0.010 86	8.547E−5	−2.633E−7	2.854E−10	−1.851E−13
0.375	0.442 3	0.089 27	0.223 6	−0.034 04	0.000 2961	−1.332E−6	2.255E−9	−1.513E−12
0.400	0.428 1	0.095 75	0.310 5	−0.090 23	0.000 9982	−6.417E−6	1.650E−9	−1.709E−11
0.425	0.412 3	0.098 47	0.322 7	−0.038 91	0.003 276	−2.9941E−5	1.138E−8	−1.845E−10
0.450	0.394 7	0.097 67	0.337 6	0.012 50	0.010 24	−0.000 1372	7.519E−7	−1.873E−9
0.475	0.375 2	0.093 49	0.352 2	0.060 10	0.028 76	−0.000 6282	4.837E−6	−1.802E−8
0.500	0.353 7	0.085 97	0.363 8	0.100 3	0.067 88	−0.002 696	3.076E−5	−1.677E−7
0.525	0.329 8	0.075 08	0.371 5	0.132 6	0.137 7	−0.016 6	0.000 1963	−1.539E−6
0.550	0.303 4	0.060 66	0.375 6	0.158 0	0.226 7	−0.042 7	0.001 266	−1.419E−5
0.575	0.273 9	0.042 50	0.376 3	0.177 5	0.255 9	0.018 7	0.007 867	−0.000 1346
0.600	0.241 1	0.020 25	0.373 7	0.191 5	0.285 7	0.077 9	0.037 80	−0.001 367
0.625	0.204 3	−0.006 551	0.367 7	0.200 2	0.309 2	0.126 2	0.123 5	−0.020 40
0.650	0.162 7	−0.038 54	0.358 1	0.203 8	0.326 4	0.164 5	0.197 7	0.004 876
0.675	0.115 5	−0.076 58	0.344 4	0.202 0	0.337 8	0.193 9	0.242 3	0.077 72
0.700	0.061 44	−0.121 8	0.326 1	0.194 6	0.343 4	0.215 2	0.277 5	0.136 4
0.725	−0.001 109	−0.175 7	0.302 6	0.180 9	0.343 2	0.228 7	0.303 3	0.181 7
0.750	−0.074 36	−0.240 6	0.272 5	0.159 9	0.336 6	0.234 0	0.320 3	0.215 1
0.775	−0.161 4	−0.319 3	0.234 3	0.130 2	0.322 7	0.230 6	0.328 4	0.237 1
0.800	−0.266 8	−0.416 4	0.185 5	0.089 36	0.300 0	0.217 3	0.327 0	0.247 6
0.825	−0.397 4	−0.538 5	0.122 4	0.033 80	0.265 9	0.191.7	0.314 6	0.245 3
0.850	−0.488 0	−0.614 0	0.077 54	−0.000 5504	0.243 7	0.180 0	0.335 7	0.279 5

or

$$\tilde{\tau}_n^e = \tilde{\mu}_n^e q^{-1/2}\left(\frac{n}{n+1}\right). \tag{19b}$$

Equivalently, $\tilde{\tau}_n^e$ are the asymptotic estimates for the zeros of the ordinary first derivative $e_q'(x) \equiv \mathrm{d}e_q(x)/\mathrm{d}x$. An improved estimate for the nth zero is obtained by solving the associated asymptotic polynomial:

$$\tilde{\tau}_n^e = \left(\frac{q^{-n/2}}{1-q}\right) y_n$$

$$1 + \sum_{m=1}^{2n-1} p^{m(m-2n+1)}(m+1)y^m = 0. \tag{20}$$

The asymptotic formula for the inflection points, i.e. for the zeros of the second derivative $e_q''(x) = \mathrm{d}^2 e_q(x)/\mathrm{d}^2 x$, is

$$\tilde{i}_n^e = -\frac{q^{-(n+1)/2}}{1-q}\left(\frac{n}{n+2}\right). \tag{21a}$$

For the rth derivative of $e_q(x)$, the asymptotic formula for the zeros is ($r \geqslant 1$; $n = 1, 2, \ldots$)

$$x_n^{(r)} = -\frac{q^{-(n+r-1)/2}}{1-q}\left(\frac{n}{n+r}\right). \tag{21b}$$

The improved estimate is

$$x_n^{(r)} = \frac{p^{-2(n+r-1)}}{1-q} y_n^{(r)} \tag{21c}$$

with the asymptotic polynomial

$$r! + \sum_{m=1}^{2n-1} p^{m(m-2n+1)}(m+r)(m+r-1)\ldots(m+1)y^m = 0. \tag{21d}$$

In the same manner, we consider the indefinite integral

$$\begin{aligned} e_q^{(-1)}(x) &\equiv \int^x e_q(y)\,\mathrm{d}y + \text{constant} \\ &= x + \frac{x^2}{2[1]!} + \frac{x^3}{3[2]!} + \ldots \\ &= \sum_{n=0}^{\infty} \frac{x^{n+1}}{(n+1)[n]!} \end{aligned} \tag{22}$$

where the constant has been chosen so $e_q^{(-1)}(0) = 0$. The asymptotic 'zeros' of $e_q^{(-1)}(x)$ are at $\tilde{z}_0^{(-1)} = 0$ and for $n = 1, 2, \ldots$ at

$$\tilde{z}_n^{(-1)} = -\frac{q^{-(n-1)/2}}{1-q}\left(\frac{n+1}{n}\right). \tag{23a}$$

For the rth indefinite integral of $e_q(x)$, the asymptotic formula for the zeros is ($r \geqslant 1$; $n = 1, 2, \ldots$)

$$x_n^{(-r)} = -\frac{q^{-(n-1)/2}}{1-q}\binom{n+r}{n}. \tag{23b}$$

The improved estimate is

$$x_n^{(-r)} = -\frac{p^{-2(n-1)}}{1-q}\, y_n^{(-r)} \tag{23c}$$

with the asymptotic polynomial

$$\frac{1}{r!} + \sum_{m=1}^{2n-1} \frac{p^{m(m-2n+1)}}{(m+r)(m+r-1)\ldots(m+1)}\, y^m = 0. \tag{23d}$$

Figure 3 displays the indefinite integral of $e_q(x)$, $e_q(x)$ itself, and its first and second derivatives.

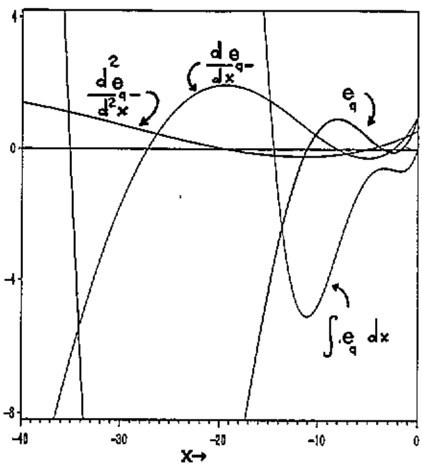

Figure 3. Plot for $q = 0.1$ showing the indefinite integral of $e_q(x)$, $e_q(x)$ itself, and its first and second derivatives. Each shows the same universal behaviour, except that the first collision point $q_1^{(-1)*}$ has already occurred for the indefinite integral of $e_q(x)$.

In summary, we define the set of functions for 'r' a positive integer:

$$\text{(i)}\quad e_q^{(r)}(x) = \frac{\mathrm{d}^r}{\mathrm{d}x^r} e_q(x) \tag{24a}$$

$$= \sum_{n=r}^{\infty} \frac{n(n-1)\ldots(n-r+1)x^{n-r}}{[n]!}$$

$$= \sum_{n=r}^{\infty} \frac{n!}{(n-r)!}\frac{x^{n-r}}{[n]!} \tag{24b}$$

where $e_q^{(0)}(x)=e_q(x)$. Note that $e_q^{(1)}(0)=1$ but that the normalization for $e_q^{(r)}(0)$, $r\neq 1$, is fixed by the definition (24*a*).

$$\text{(ii)}\quad e_q^{(-r)}(x)=\int^x \mathrm{d}x_1 \int^{x_1} \mathrm{d}x_2 \ldots \int^{x_{r-1}} \mathrm{d}x_r e_q(x_r)+\text{constant} \tag{25a}$$

$$=\sum_{n=0}^{\infty} \frac{1}{(n+r)(n+r-1)\ldots(n+1)} \frac{x^{n+r}}{[n]!}$$

$$=\sum_{n=0}^{\infty} \frac{n!}{(n+r)!} \frac{x^{n+r}}{[n]!}. \tag{25b}$$

Note that as $q\to 1$, $e_q^{(r)}(x)\to\exp(x)$. The constant(s) in (25) have been chosen for simplicity so $e_q^{(-r)}(0)=0$. Consequently, $e_q^{(-r)}(x)\not\to\exp(x)$ as $q\to 1$ since the $e_q^{(-r)}$ series begins with order x^r terms. *A different choice of the constants can be easily made if needed in applications*. Each $e_q^{(\pm r)}(x)$ is entire and has an essential singularity at infinity.

3. Properties of zeros of $e_q(x)$ as q increases

At a q value of $q_1^*\approx 0.14$, we find numerically that the first two zeros z_1 and z_2 of $e_q(x)$ collide at $x_1^*\approx -2.48$ and move off the negative real axis into the complex z plane. They move off as (and remain) a complex conjugate pair. As q increases, this occurs again for the associated-pair z_3 and z_4, etc. This behaviour of $e_q(x)$ is quantitatively summarized in the following tables and plots. We also find, from figure 3 and table 2, that a similar collision process occurs for the indefinite integral and first two derivatives of $e_q(x)$.

Note that *this similar behavior* for $x<0$ *of the zeros* of the various $e_q^{(\pm r)}(x)$ functions is not so surprising. The analytic e_q function has an infinite number of zeros for $x<0$ which asymptotically go as $\tilde{\mu}_n$. Each of the entire $e_q^{(\pm r)}$ functions is defined by an infinite (convergent) alternating series, for $x<0$, and these series are related differentially. Thus, between successive zeros of $e_q^{(r)}$ there must be a smooth maximum (or minimum) which is the location of a zero of $e_q^{(r+1)}$. The simplest case is that there are no other relative maxima (or minimum) between such successive zeros. For $r>0$, this intertwining of *the zeros of* $e_q^{(r)}$ *with those of* $e_q^{(r+1)}$ *in association with* $e_q^{(r)}(x)\to\exp(x)$ *as* $q\to 1$ makes a common pairwise collision process the simplest option for the disappearance of the real zeros as $q\to 1$ (for instance, this intertwining prevents the zeros from going off to negative real infinity as $q\to 1$). We find no numerical evidence for any of the $e_q^{(\pm r)}$ functions that additional collisions among the zeros occur off the real axis in the compelx z plane. A remark is also due on the properties $e_q^{(-r)}(x)$ in the negative x region near the origin. The presence and location (in q^* and x^*) of the zeros, and also the sign of $e_q^{(-r)}(x)$ at its turning points, is affected by the choice of normalization, $e_q^{(-r)}(0)=0$.

Table 2 lists the q^* and x^* values for the first five collision points for the four functions shown in figure 3.

Recall that we label the zeros of $e_q(x)$ by

$$z_n=\mu_n+\mathrm{i}\nu_n. \tag{26}$$

The real parts μ_n for the first 10 zeros are tabulated in table 3 and plotted in figure 4. For these real parts, the plot of figure 5 shows the asymptotic $\tilde{\mu}_n$ versus the numerically obtained μ_n. Previously in table 1 this comparison was made by listing the fractional deviations. The magnitudes of the imaginary parts ν_n for the first 10 zeros are tabulated

Table 2. q^* and x^* values for the first five collision points for, respectively, the indefinite integral of $e_q(x)$, for $e_q(x)$ itself, and for its first and second derivatives. In the case of the indefinite integral of $e_q(x)$, for $n=1$ (and 4) the (daggered) values shown are remarkable in that $\mu_1=\mu_2$ (and $\mu_7=\mu_8$) for 20 significant figures.

n	q_n^*	x_n^*
1	0.056†	−4.572 40
2	0.237 423	−11.334 1
3	0.384 120	−17.755 6
4	0.488 124†	−24.042 5
5	0.563 479	−30.272 2
1	0.140 756 658	−2.479 81
2	0.388 476 941	−6.067 19
3	0.536 570 493	−9.536 38
4	0.628 767 521	−12.968 9
5	0.690 878 670	−16.385 1
1	0.251 977	−3.488 18
2	0.458 251	−6.994 55
3	0.579 584	−10.439 6
4	0.657 398	−13.862 0
5	0.711 185	−17.273 8
1	0.338 992	−4.420 97
2	0.512 004	−7.905 90
3	0.614 215	−11.340 2
4	0.681 284	−14.756 6
5	0.728 579	−18.164 8

in table 4 and plotted in figure 6. Note that in the q range shown in figure 6, the $n=1$ curve for $|\nu_1|$ in figure 6 crosses over two higher-n curves, and the $n=3$ curve for $|\nu_3|$ crosses over one higher-n curve.

For completeness, figures 7 and 8 contain plots of the polar coordinates of the first eight zeros. We define

$$\rho_n \equiv \sqrt{\mu_n^2+\nu_n^2} \tag{27}$$

$$\phi_n \equiv \tan(|\nu_n/\mu_n|) \tag{28}$$

where $\phi_n=0$ labels the negative real axis.

4. Properties of $e_q(z)$ in the complex z plane

We have numerically studied the properties of $\mathrm{Re}\{e_q(z)\}$ and of $\mathrm{Im}\{e_q(z)\}$ in the complex z plane as q is varied. This behaviour is partially discernible from the discussion of $e_q(x)$ in sections 2 and 3, and from Exton's paper [1] on the properties of

$$\cos_q(y) \equiv \mathrm{Re}\{e_q(\mathrm{i}y)\} = \sum_{n=0}^{\infty} (-)^n \frac{y^{2n}}{[2n]!} \tag{29a}$$

Table 3. μ_n for the first 10 zeros of $e_q(z)$. An asterisk in a column denotes the same value as entered to the immediate left. An asterisk on the left edge denotes that it is a collision point row, except at =0.700 where it is the row nearest to $q_5^{\dagger}=0.690\,87\ldots$.

	q	z_1	z_2	z_3	z_4	z_5	z_6	z_7	z_8	z_9	z_{10}
	0.100	−1.742 69	−3.394 91	−11.112 1	−35.112 1	−111.111	−351.364	−1111.11	−3513.64	−11111.1	−35136.4
	0.125	−2.020 42	−2.977 13	−9.145 70	−25.859 9	−73.142 9	−206.879	−585.143	−1655.03	−4681.14	−13240.3
*	0.141	−2.479 82	*	−8.273 32	−22.038 4	−58.741 6	−156.571	−417.327	−1112.35	−2964.89	−7902.66
	0.150	−2.475 44	*	−7.850 05	−20.250 9	−52.287 6	−135.006	−348.584	−900.040	−2323.89	−6000.26
	0.175	−2.483 07	*	−6.941 73	−16.557 2	−39.579 5	−94.613 0	−226.168	−540.646	−1292.39	−3089.40
	0.200	−2.512 43	*	−6.281 74	−13.975 2	−31.250 0	−69.877 1	−156.250	−349.386	−781.250	−1746.93
	0.225	−2.556 73	*	−5.796 96	−12.089 2	−25.487 9	−53.733 1	−113.279	−238.814	−503.464	−1061.39
	0.250	−2.609 87	*	−5.448 89	−10.664 7	−21.333 3	−42.666 7	−85.333 3	−170.667	−341.333	−682.667
	0.275	−2.666 19	*	−5.218 77	−9.559 44	−18.238 8	−34.780 1	−66.323 0	−126.473	−241.174	−459.902
	0.300	−2.721 35	*	−5.098 62	−8.681 31	−15.873 1	−28.980 0	−52.910 1	−96.600 1	−176.367	−322.000
	0.325	−2.773 35	*	−5.087 54	−7.964 50	−14.026 2	−24.603 0	−43.156 5	−75.701 5	−132.789	−232.928
	0.350	−2.822 21	*	−5.197 55	−7.350 08	−12.559 9	−21.228 4	−35.882 5	−60.652 5	−102.521	−173.293
	0.375	−2.868 88	*	−5.495 40	−6.738 05	−11.381 1	−18.579 8	−30.340 7	−49.546 2	−80.908 6	−132.123
*	0.388	−2.893 47	*	−6.067 21	*	−10.841 9	−17.384 9	−27.892 8	−44.751 6	−71.800 3	−115.198
	0.400	−2.914 29	*	−6.042 85	*	−10.427 1	−16.470 1	−26.041 7	−41.175 5	−65.104 2	−102.939
	0.425	−2.959 08	*	−6.041 85	*	−9.660 06	−14.768 9	−22.655 1	−34.751 3	−53.306 0	−81.767 7
	0.450	−3.003 76	*	−6.099 31	*	−9.071 59	−13.382 8	−19.952 6	−29.743 6	−44.339 1	−66.096 9
	0.475	−3.048 75	*	−6.190 41	*	−8.692 16	−12.241 5	−17.773 1	−25.787 7	−37.416 8	−54.290 0
	0.500	−3.094 47	*	−6.287 60	*	−8.582 56	−11.280 2	−16.000 5	−22.627 4	−32.000 0	−45.254 8
	0.525	−3.141 38	*	−6.380 14	*	−8.857 98	−10.369 4	−14.551 7	−20.079 3	−27.712 1	−38.246 3
*	0.537	−3.163 62	*	−6.421 99	*	−9.536 62	*	−13.974 6	−19.068 7	−26.032 1	−35.538 2
	0.550	−3.189 95	*	−6.470 41	*	−9.499 96	*	−13.373 6	−18.009 9	−24.284 9	−32.745 7
	0.575	−3.240 69	*	−6.560 97	*	−9.564 23	*	−12.474 9	−16.319 8	−21.524 9	−28.386 1
	0.600	−3.294 20	*	−6.653 08	*	−9.722 50	*	−12.028 8	−14.921 7	−19.290 5	−24.903 4
	0.625	−3.351 14	*	−6.748 04	*	−9.882 77	*	−12.462 0	−13.540 0	−17.480 7	−22.105 7
*	0.629	−3.360 07	*	−6.762 69	*	−9.906 31	*	−12.968 9	*	−17.240 9	−21.734 3
	0.650	−3.412 32	*	−6.847 37	*	−10.039 0	*	−12.967 6	*	−16.069 2	−19.851 4
	0.675	−3.478 72	*	−6.952 86	*	−10.197 4	*	−13.203 6	*	−15.443 5	−18.005 7
*	0.700	−3.551 54	*	−7.066 68	*	−10.360 8	*	−13.450 1	*	−16.352 2	*
	0.725	−3.632 34	*	−7.191 51	*	−10.533 2	*	−13.696 0	*	−16.649 0	*
	0.750	−3.723 14	*	−7.330 83	*	−10.719 3	*	−13.949 1	*	−17.005 4	*
	0.775	−3.826 70	*	−7.489 29	*	−10.925 4	*	−14.217 3	*	−17.364 1	*
	0.800	−3.946 87	*	−7.673 37	*	−11.160 3	*	−14.511 3	*	−17.738 7	*
	0.825	−4.089 23	*	−7.892 46	*	−11.436 2	*	−14.847 0	*	−18.121 8	*
	0.850	−4.262 36	*	−8.161 00	*	−11.771 9	*	−15.251 4	*	−18.569 8	*

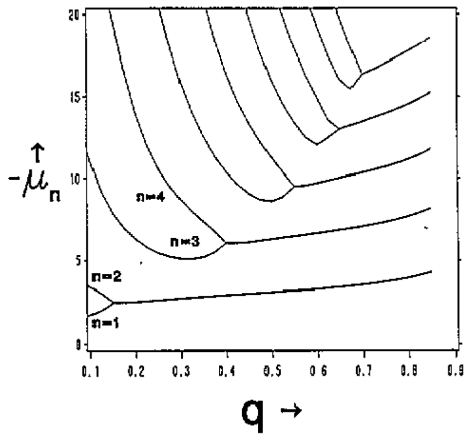

Figure 4. Plot of the real parts of the first 10 zeros, $z_n = \mu_n + i\nu_n$, near their collision points.

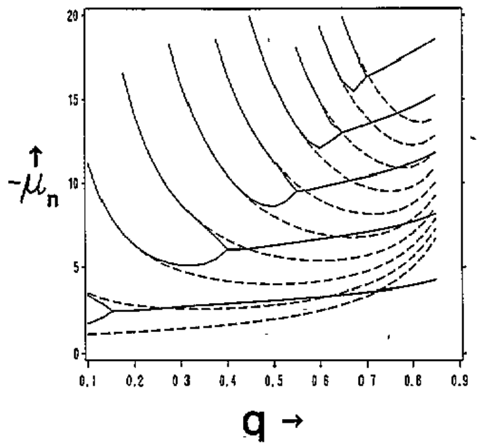

Figure 5. Plot showing the asymptotic expression, $\tilde{\mu}_n$, for the real parts of the first 10 zeros versus the numerically obtained real parts.

Table 4. $|\nu_n|$ for the first 10 zeros of $e_q(x)$.

q	$z_{1,2}$	$z_{3,4}$	$z_{5,6}$	$z_{7,8}$	$z_{9,10}$
0.150	0.350 962	0	0	0	0
0.175	0.661 285	0	0	0	0
0.200	0.866 821	0	0	0	0
0.225	1.045 74	0	0	0	0
0.250	1.219 67	0	0	0	0
0.275	1.397 33	0	0	0	0
0.300	1.581 51	0	0	0	0
0.325	1.772 28	0	0	0	0
0.350	1.969 42	0	0	0	0
0.375	2.173 56	0	0	0	0
0.388	2.286 97	0	0	0	0
0.400	2.386 06	0.570 555	0	0	0
0.425	2.608 73	1.031 16	0	0	0
0.450	2.843 55	1.393 27	0	0	0
0.475	3.092 80	1.759 48	0	0	0
0.550	3.359 07	2.151 54	0	0	0
0.525	3.645 45	2.565 99	0	0	0
0.537	3.785 80	2.764 96	0	0	0
0.550	3.955 65	3.002 31	0.830 746	0	0
0.575	4.294 22	3.465 58	1.501 30	0	0
0.600	4.666 74	3.962 18	2.158 82	0	0
0.625	5.080 26	4.499 65	2.874 79	0	0
0.629	5.146 66	4.584 76	2.986 68	0	0
0.650	5.543 77	5.087 57	3.639 39	1.380 73	0
0.675	6.068 97	5.738 27	4.465 87	2.405 35	0
0.700	6.671 36	6.468 06	5.371 50	3.536 62	1.055 21
0.725	7.371 99	7.298 97	6.379 13	4.768 31	2.534 83
0.750	8.200 24	8.261 59	7.520 46	6.134 58	4.172 17
0.775	9.198 37	9.399 78	8.840 78	7.681 88	5.990 48
0.800	10.429 5	10.778 9	10.407 4	9.479 17	8.064 44
0.825	11.992 6	12.500 9	12.324 9	11.634 0	10.497 8
0.850	14.052 0	14.734 7	14.766 5	14.306 9	13.923 4

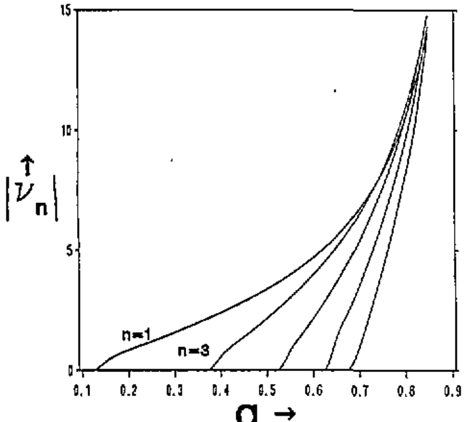

Figure 6. Plot of the magnitude of the imaginary parts of the first 10 zeros, $z_n = \mu_n + \mathrm{i}\nu_n$, near their collision points. The subscript n labels the first (odd#) zero of the associate pair.

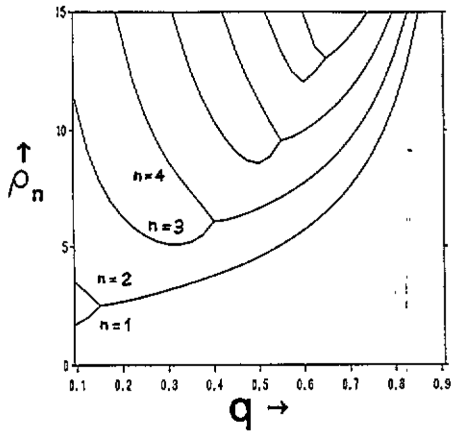

Figure 7. Plot of the polar part, $\rho_n = \sqrt{\mu_n^2 + \nu_n^2}$, of the first eight zeros near their collision points.

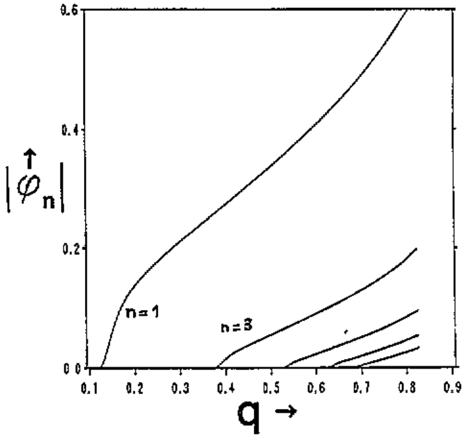

Figure 8. Plot of the magnitudes of the arguments of the first 10 zeros, $\phi_n \equiv \tan^{-1}(|\nu_n/\mu_n|)$. Note that $\phi_n = 0$ specifies the negative real axis.

and

$$\sin_q(y) \equiv \mathrm{Im}\{e_q(\mathrm{i}y)\} = \sum_{n=0}^{\infty} (-)^n \frac{y^{2n+1}}{[2n+1]!} \tag{29b}$$

as q is varied. Here y is a real variable. These functions are respectively even and odd in y.

These q-analogue trigonometric functions are related by the q-derivative operation where a = 'constant independent of x'

$$\frac{\mathrm{d}}{\mathrm{d}_q x} \sin_q(ax) = a \cos_q(ax) \tag{30a}$$

$$\frac{\mathrm{d}}{\mathrm{d}_q x} \cos_q(ax) = -a \sin_q(ax) \tag{30b}$$

where

$$\frac{\mathrm{d}}{\mathrm{d}_q x} f(x) \equiv \frac{f(q^{1/2}x) - f(q^{-1/2}x)}{q^{1/2}x - q^{-1/2}x}. \tag{30c}$$

They likewise satisfy the obvious (inverse) q-integration relation. Exton [1, 10] has studied q-orthogonality properties they possess. For $\cos_q(y)$, $y \geqslant 0$, the asymptotic zeros [1] and turning points are for $n^c = 1, 2, 3, \ldots$

$$\tilde{\mu}_n^c = \frac{q^{3/4-n}}{1-q}$$
$$\tilde{\tau}_n^c = \pm \frac{q^{-n-1/4}}{(1-q)} \left(\frac{n}{n+1}\right)^{1/2} \tag{31}$$

and $\tilde{\tau}_0^c = 0$. For $\sin_q(y)$ for $y > 0$ they are for $n^s = 1, 2, 3, \ldots$ ($\tilde{\mu}_0^s = 0$)

$$\tilde{\mu}_n^s = \frac{q^{1/4-n}}{1-q}$$
$$\tilde{\tau}_n^s = \frac{q^{1/4-n}}{1-q} \left(\frac{2n-1}{2n+1}\right)^{1/2}. \tag{32}$$

So for both q-trigonometric functions, as $|y|$ increases the frequency of oscillation decreases, and the amplitude is found to increase. Numerically we find for fixed q that as $n \to \infty$ the fractional deviations of (31)–(32) from the actual values decrease monotonically. We have not found any numerical indication of possible non-real zeros for $\cos_q(z)$ or for $\sin_q(z)$ for z complex. (If desired, the associated asymptotic polynomials and ordinary higher derivatives and higher-indefinite integrals can be obtained by the reader for these two functions).

To display the behaviour of $e_q(z)$ in the complex z plane, we set $q = 0.35$, which is after the collision point at $q_1^* \approx 0.14$. Figure 9 shows the contour plot for $\mathrm{Re}\{e_q(z)\}$, and figure 10 that for $\mathrm{Im}\{e_q(z)\}$. The graphical notation in these two figures is explained in their captions.

As q increases beyond 0.35 towards 1, each associated pair of zeros similarly collides as discussed in section 3 and moves off into the complex z plane. This numerically studied flow is consistent with the limiting behaviours as $q \to 1$,

$$\mathrm{Re}\{e_q(z)\} \to \mathrm{Re}\{\exp(z)\} = \mathrm{e}^x \cos y \tag{33a}$$

$$\mathrm{Im}\{e_q(z)\} \to \mathrm{Im}\{\exp(z)\} = \mathrm{e}^x \sin y \tag{33b}$$

displayed, for the reader's convenience, in the top row of figure 11. Likewise, as $q \to 0$ it is evident how figures 9 and 10 change smoothly into the bottom row of figure 11 showing $\mathrm{Re}(1+z) = 1+x$ and $\mathrm{Im}(1+z) = y$ in the same graphical notation.

If for x real we define the q-analogue hyberbolic functions

$$\cosh_q(x) \equiv 1/2\{e_q(x) + e_q(-x)\} = \cos_q(\mathrm{i}x)$$
$$= \sum_{n=0,2,\ldots}^{\infty} \frac{x^n}{[n]!} \tag{34a}$$

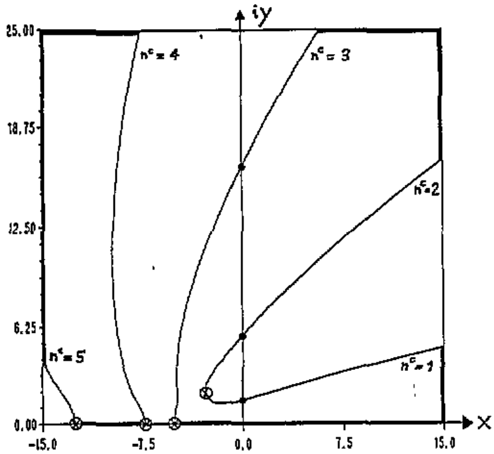

Figure 9. A 'contour plot' of $\mathrm{Re}\{e_q(z)\}$ in the complex $z=x+iy$ plane for $q=0.35$, which is after the first collision. The zeros of $e_q(z)$ are at the 'crossed-circle points'. The 'solid circle points' along the imaginary axis show the zeros of $\cos_q(y)=\mathrm{Re}\{e_q(iy)\}$. An n^c value labels each of these zeros, and also labels the contour lines which show where $\mathrm{Re}\{e_q(z)\}=0$. Heavy black borders display the regions where $\mathrm{Re}\{e_q(z)\}>0$.

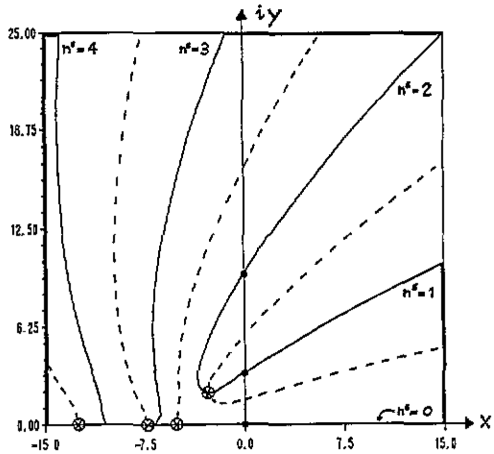

Figure 10. A 'contour plot' of $\mathrm{Im}\{e_q(z)\}$ in the complex z plane for $q=0.35$. Here, the 'solid circle points' along the imaginary axis show the zeros of $\sin_q(y)=\mathrm{Im}\{e_q(iy)\}$. An n^s value labels the $\sin_q(y)$ zeros, and also labels contour lines which show where $\mathrm{Im}\{e_q(z)\}=0$. Heavy black borders show the regions where $\mathrm{Im}\{e_q(z)\}>0$. The broken contour lines show the $\mathrm{Re}\{e_q(z)\}=0$ contours overlaid from figure 9.

$$\begin{aligned}\sinh_q(x) &\equiv 1/2\{e_q(x)+e_q(-x)\} = -\mathrm{i}\sin_q(\mathrm{i}x)\\ &= \sum_{n=1,3,\ldots}^{\infty} \frac{x^n}{[n]!}\end{aligned} \tag{34b}$$

these even/odd functions are simply flatter counterparts of the usual ones; for instance, for $x>0$ they are both monotonic. Again

$$\frac{\mathrm{d}}{\mathrm{d}_q x}\cosh_q(ax) = a\sinh_q(ax) \qquad \frac{\mathrm{d}}{\mathrm{d}_q x}\sinh_q(ax) = a\cosh_q(ax). \tag{35}$$

In terms of figures 1 and 2 they have a simple interpretation. Recall the $e_q(x)$ bound that $|e_q(x)| \leqslant e_q(|x|)$, so the distance of $e_q(x)$ below this upper bound for $x<0$ is

$$\begin{aligned}\mathrm{d_b} &\equiv e_q(|x|) - e_q(x)\\ &= -2\sinh_q(x) \qquad x<0.\end{aligned} \tag{36a}$$

Likewise, the distance above this lower bound for $x<0$ is

$$\begin{aligned}\mathrm{d_a} &\equiv e_q(x) - \{-e_q(|x|)\}\\ &= 2\cosh_q(x).\end{aligned} \tag{36b}$$

So, in general this bound is a very poor envelope for $e_q(x)$.

5. The reciprocal function $e_q^{-1}(z)$

By the Hadamard–Weierstrass factorization theorem, [12] we can obtain the infinite product representation for $e_q(x)$ for $0 \leqslant q < 1$. We first use the expression for $\log([n]_q!)$

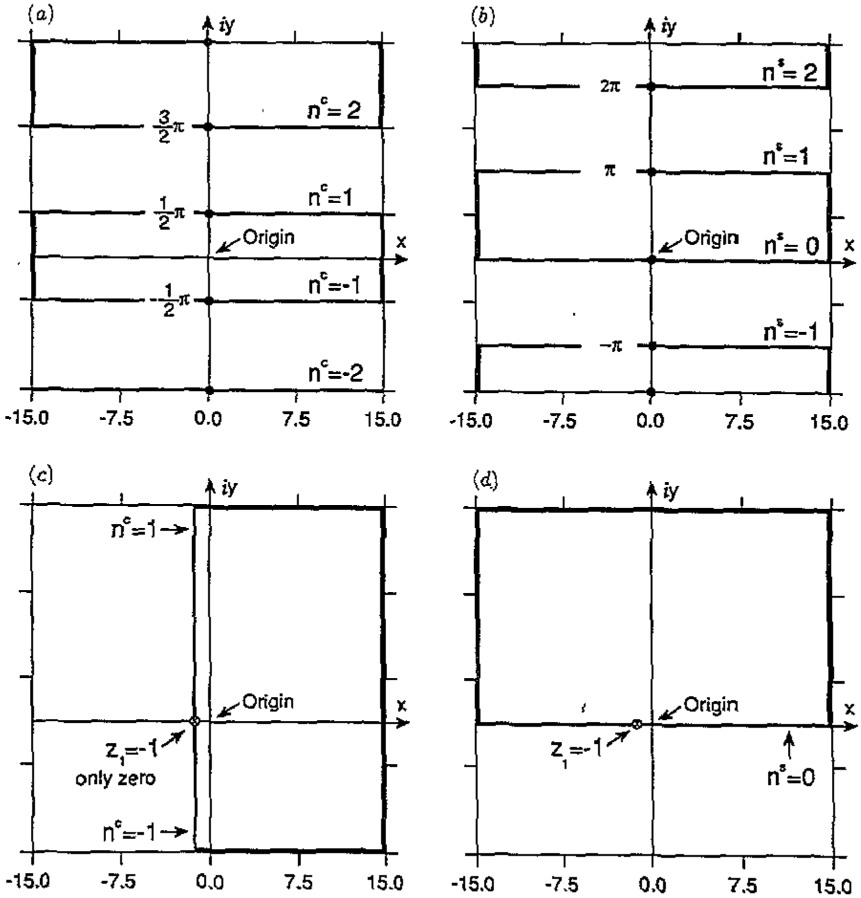

Figure 11 Contour plots of the complex function $e_q(z)$ for the limiting caes $q=1$ (top row) and for $q=0$ (bottom row) for comparison with the previous two figures. The first column, (*a*) and (*c*), show $\mathrm{Re}\{e_q(z)\}$ and the second column, (*b*) and (*d*), show $\mathrm{Im}\{e_q(z)\}$. The labelling is respectively as for figures 9 and 10.

preceding (14*b*) to calculate the order ρ of the entire function $e_q(z)$. If the entire function $f(z)$ is of order ρ, then

$$f(z)=\mathrm{O}\{\exp(r^{\rho+\varepsilon})\}$$

as $|z|=r\to\infty$, for every $\varepsilon>0$, but not for any $\varepsilon<0$. Every polynomial is of order zero; for order zero entire functions

$$f(z)\to\mathrm{O}\{\exp(r^{\varepsilon})\}$$

as $|z|=r\to\infty$. The standard formula for the order $\rho(f)$ for $f(z)=\Sigma_{n=0}^{\infty} c_n z^n$ is [12]

$$\begin{aligned}\rho\{e_q(z)\}&=\lim_{n\to\infty}\sup\frac{n\log n}{\log|1/c_n|}\\&=\lim_{n\to\infty}\sup\frac{n\log n}{\log([n]_q!)}\end{aligned}$$

where by (14b)

$$\log([n]_q!) = n\{(n-1)|\log p| + |\log(1-q)|\} + r_n.$$

The remainder, which arises from the second 'braces' factor in (14b), is

$$r_n = \sum_{m=1}^{n} \log(1-q^m) < 0.$$

It is bounded by

$$|r_n| \leqslant n|\log(1-q)|.$$

Therefore, the order

$$\rho\{e_q(z)\} \leqslant \left\{\limsup_{n\to\infty} \frac{n\log n}{n(n-1)|\log p|} = 0\right\}.$$

Hence, for every q, $0 \leqslant q < 1$, $e_q(z)$ is an entire function of order 0. For $0 < q < 1$, $e_q(z)$ is not a polynomial, so it has infinitely many zeros. With $z_1, z_2, \ldots$ equal to the zeros (listed in order of increasing magnitude), the product representation is [12] (since $e_q(0) = 1$)

$$e_q(z) = \prod_{n=1}^{\infty} (1 - z/z_n) \qquad q \neq 1 \tag{37}$$

where $z_n = \mu_n + \mathrm{i}\nu_n$ is the nth zero of $e_q(x)$. Therefore, the reciprocal function can also be written as an infinite product

$$e_q^{-1}(z) = \prod_{n=1}^{\infty} (1 - z/z_n)^{-1} \qquad q \neq 1 \tag{38}$$

where $e_q^{-1}(z)e_q(x) = 1$. Also for all $\varepsilon > 0$, the series

$$\sum_{n=1}^{\infty} \frac{1}{|z_n|^{\varepsilon}}$$

converges, i.e. the exponent of convergence of the sequence $\{z_n\}$ is zero.

By multiplying out the product in (37), a sum rule for the zeros of $e_q(z)$ follows:

$$\sum_{n=1}^{\infty} (1/z_n) = -1 \qquad q \neq 1. \tag{39}$$

In a separate paper, we will report on the higher-order sum rules for the zeros which follow from (37). (We have checked (39) numerically for $\sim 0.1 < q < \sim 0.8$.)

Similarly, it is straightforward to directly show that the following functions are also order zero for $0 \leqslant q < 1$: $e_q^{(r)}(z)$, $e_q^{(-r)}(z)$, $\cos_q(z)$ and $\sin_q(z)$. Hence, since the usual $\exp(z)$, $\cos(z)$ and $\sin(z)$ functions are of order 1, the order of these q-analogue entire functions is discontinuous in the limit $q \to 1$.

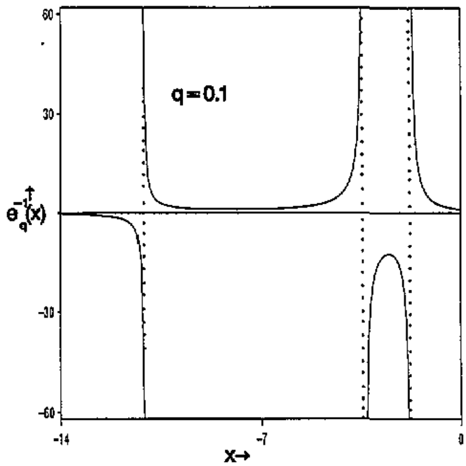

Figure 12. Plot showing the universal behaviour of the reciprocal function $e_q^{-1}(z)$ for $q<q_1^*$ ($q_1^* \approx 0.14$). The simple poles at z_n with $n=1,2,\ldots$ are shown by vertical broken lines.

Figure 12 shows the universal behaviour of e_q^{-1} for $x<0$ and $q<q_1^*$ ($q_1^* \approx 0.14$). As q is increased beyond $q_1^* \approx 0.14$, the pair-associated simple poles of e_q^{-1} collide and move off into the complex z plane, etc. The discussion and figures 9–11 of section 3 for the properties of the zeros of $e_q(x)$ can be easily reinterpreted in terms of the poles of $e_q^{-1}(z)$. For example, the 'crossed-circle points' in these figures now show the location of the simple poles of $e_q^{-1}(z)$. For special q values, i.e. the collision points q_n^*, $e_q^{-1}(z)$ does have a single double pole at $z=x_n^*$ on the negative real axis. For $q<q_1^*$, the infinite number of simple poles of $e_q^{-1}(z)$ lie only on the negative real axis.

Acknowledgments

One of us (CAN) wishes to thank M Fields, Z Yu and C Zachos for discussions. He thanks Robert F Riley for helpful discussions. He thanks the theory group at Cornell for intellectual stimulation. This work was partially supported by the US Department of Energy, Contract No. DE-FG02-86ER40291.

Appendix 1. Properties of $E_q(z)$

For completeness, we briefly compare some of the analogous results [11, 2] for the alternative realization [13, 14] of the q-boson commutation relations in which b and b^+ satisfy

$$bb^+ - qb^+b = 1.$$

where $0<q<\infty$. Consequently the remaining 'type a' realization listed in [13] is no different from this 'type b' realization. 'Type a' is only a relabelling $q \to 1/q$ with $b \to a$, $b^+ \to a^+$ so

$$aa^+ - q^{-1}a^+a = 1.$$

The q-cs are defined [14] by

$$|z\rangle_J = \{E_q(|z|^2)\}^{-1/2} \sum_{n=1}^{\infty} \frac{z^n}{\sqrt{[n]_J!}} |n\rangle$$

for $0<q<1$; $[n]_J$ is defined below. The q-boson transformation [13] from the upper equation in (4) to above realization is $b=q^{N/4}a, b^+=a^+q^{N/4}$. The associated q-boson completeness relation [14] is

$$\int \mathrm{d}\mu(z)|z\rangle_{J\,J}\langle z| = 1$$

with

$$\mathrm{d}\mu(z) = (1/2\pi)E_q(|z|^2)E_{1/q}(-q|z|^2)\,\mathrm{d}_q|z|^2\,\mathrm{d}\theta \qquad 0<q<1$$

and $|z|^2 \leqslant \zeta_J$. Here also it is the $E_{1/q}(-q|z|^2) = \{E_q(q|z|^2)\}^{-1}$ factor that is important in the measure.

Figures 13 and 14 show the plots, respectively for $q \geqslant 1$ and $0<q<1$, of Jackson's q-exponential function [11]

$$E_q(x) = \sum_{n=0}^{\infty} x^n/[n]_J! \qquad [n]_J \equiv \frac{1-q^n}{1-q}.$$

For $q \geqslant 1$, this series converges uniformly and absolutely for all finite z. There is an essential singularity at infinity. The oscillations increase in amplitude as $x \to (-\infty)$.

The properties of $E_q(x)$ for $q>1$ appear qualitatively the same as those of $e_q(x)$ for q less than the first collision point at $q_1^* \approx 0.14$. *Since $e_q(x)$ is symmetric under $q \leftrightarrow 1/q$, the just cited properties of $e_q(x)$ reported in the text also hold for* $q > \{1/q_1^*\}$ where $1/q_1^* \approx 7.1$.

However, the zeros of $E_q(x)$ for $q>1$ do not collide pairwise as $q \to 1$ but instead move off to infinity so that $E_q(z) \to \exp(z)$ as $q \to 1$. Also, as for $e_q(z)$, when $q \to \infty$ a

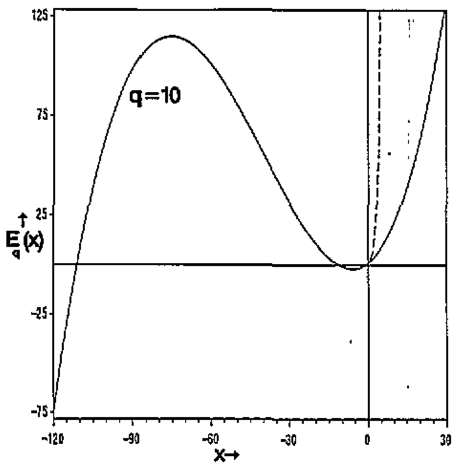

Figure 13. Plot showing the universal behaviour of Jackson's $E_q(z)$ for $q>1$. The broken curve for x positive is $\exp(x)$. The zeros are exactly at $\mu_n^E = -q^n/(q-1)$; $n=1, 2, \ldots$. So as $q \to 1$ these zeros move off to negative infinity.

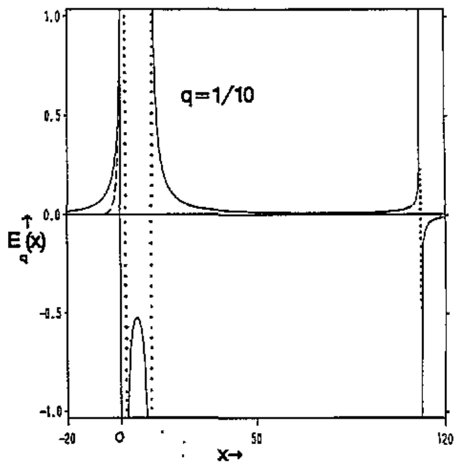

Figure 14. Plot showing the universal behaviour of $E_q(x)$ for $q<1$. The broken curve for x negative is $\exp(x)$. The simple poles at $q^{-n}/(1-q)$ with $n=1, 2, \ldots$ are shown by vertical broken lines.

single zero remains at $z=-1$ with $E_q(z)\to 1+z$. The zeros of $E_q(x)$ are at [11]

$$\mu_n^E=q^n/(1-q)$$

for $n=1,2,\ldots$. This follows (C Zachos, unpublished) easily from the recursion relation

$$E_q(x)=[1+x(1-q^{-1})]\,E_q(x/q).$$

Iteration gives the infinite product representation

$$E_q(x)=\lim_{R\to\infty}\left\{\prod_{r=0}^{R}(1+x(1-q^{-1})q^{-r})\right\}E_q(x/q^R)$$
$$=\prod_{r=0}^{\infty}(1+x(1-q^{-1})q^{-r})$$

since for fixed $x, q>1$, $E_q(x/q^R)\to E_q(0)=1$ as $R\to\infty$. Note that the sum rule $\Sigma_{n=0}^{\infty}(1/\mu_n^E)=-1$ then follows easily since the μ_n^E form a geometric series.

A simple way (C Zachos, unpublished) to obtain the recursion relation is to solve Jackson's q-derivative result $D_q(E_q)=E_q(x)=\{E_q(qx)-E_q(x)\}/\{qx-q\}$ for $E_q(qx)$, and then let $xq\to x'$. So, such recursion relations actually just re-express the term-by-term, power series agreement that shows $D_q(E_q)$ equals E_q.

The analogous recursion relation for $e_q(x)$ has two terms:

$$e_q(x)=e_q(q^{-1}x)+x(1-q^{-1})e_q(q^{-1/2}x).$$

However, unlike for $E_q(x)$, this recursion relation does not simply yield a formula for the zeros of $e_q(x)$.

It is important that $e_q(x)$ for $q>\{1/q_1^*\}$ has 'twice' as many zeros as $E_q(z)$. This is easily seen, for by (16) the zeros of $e_q(x)$ are asymptotically at $\tilde{\mu}_n^e=-q^{(1-n)/2}/(1-q)$ *when* $0<q<1$. For comparison with the zeros of $E_q(x)$ which are at μ_n^E *for* $q>1$, we therefore substitute $q\to 1/q$ in $\tilde{\mu}_n^e$ and find that for $n=1,2,\ldots$

$$\tilde{\mu}^e_{2n-1}|_{q\to 1/q}=-\frac{q^n}{(q-1)}\qquad q>\{1/q_1^*\}$$
$$=\mu_n^E.$$

We use the notation $q\to 1/q$ on the left-hand side of this equation to denote the explicit substitution which is required (because the text considers $0<q<1$ and not $1<q<\infty$) to compare the zeros of the text's $e_q(z)$ functions with this appendices' zeros for the $E_q(z)$ functions. This same notation is used below.

For $q>1$, the $E_q(x)$ zeros, or equivalently the $E_q^{-1}(x)$ poles, do not collide because their collision partners simply do not exist. This observation is relevant to the physical significance of the different q-boson realizations.

For $0<q<1$, the series for the *meromorphic function* $E_q(x)$ converges uniformly and absolutely for $|x|<(1-q)^{-1}$, but diverges otherwise. However, for any s, $E_s(x)E_{1/s}(-x)=1$. So for $q=1/s$ with $s>1$, $E_q(x)=1/E_{1/q}(-x)$. Thus, for $0<q<1$ figure 14 follows with simple poles for $E_q(x)$ at $q^{-n}/(1-q)$ for $n=0,1,\ldots$. Since the series representation diverges at $1/(1-q)$, one must analytically continue the function for x larger than this point. Therefore, it is not paradoxical that $E_q(x)<0$ for $x>0$ and $q<1$. For $q<1$, $E_q(x)\to\exp(x)$ as $q\to 1$, and $E_q(x)\to(1-x)^{-1}$ as $q\to 0$. For comparison with $e_q^{-1}(z)$ of figure 12 in section 6, note that figure 14 can be interpreted as a plot of $E_{\bar{q}}^{-1}(x)$ except as plotted for the arguments $\bar{q}=1/q$ and $\bar{x}=-x$.

For $q>1$, the complex z plane plots for $\mathrm{Re}\{E_q(z)\}$ and for $\mathrm{Im}\{E_q(z)\}$ are qualitatively the same as the analogous ones for $e_q(z)$ for $q>\{1/q_1^*\}$ where $1/q_1^*\approx 7.1$. However, there are in general only half as many trajectories for the zeros of $E_q(z)$ as there are for $e_q(x)$. This was shown above for zeros on the real axis. For along the imaginary axis, we define [15]

$$\begin{aligned}\mathrm{Cos}_q(y) &\equiv \mathrm{Re}\{E_q(\mathrm{i}y)\} \\ &= \sum_{n=0}^{\infty}(-)^n \frac{y^{2n}}{[2n]_J!} \\ \mathrm{Sin}_q(y) &\equiv \mathrm{Im}\{E_q(\mathrm{i}y)\} \\ &= \sum_{n=0}^{\infty}(-)^n \frac{y^{2n+1}}{[2n+1]_J!}.\end{aligned}$$

For these functions there is a matrix recursion relation:

$$\begin{pmatrix}\mathrm{Cos}_q(y)\\ \mathrm{Sin}_q(y)\end{pmatrix}=\begin{pmatrix}1 & -(1-q^{-1})y\\ (1-q^{-1})y & 1\end{pmatrix}\begin{pmatrix}\mathrm{Cos}_q(y/q)\\ \mathrm{Sin}_q(y/q)\end{pmatrix}.$$

However, for $q>1$ these functions do have asymptotically half as many zeros as their respective counterparts $\cos_q(y)$ and $\sin_q(y)$ of (29). In particular, the relations between the respective asymptotic formulae for their zeros for $y\geqslant 0$ are

$$\tilde{\mu}^{\mathrm{c}}_{2n-3/4}\big|_{q\to 1/q}=\frac{q^{2n-1/2}}{q-1}=\tilde{\mu}^{\mathrm{C}}_n \qquad q\gg 1$$

and ($\tilde{\mu}^{\mathrm{S}}_o=0$)

$$\tilde{\mu}^{\mathrm{s}}_{2n-1/4}\big|_{q\to 1/q}=\frac{q^{2n+1/2}}{q-1}=\tilde{\mu}^{\mathrm{S}}_n \qquad q\gg 1.$$

For the rth derivative of $E_{1/q}(x)$, $q<1$,

$$\begin{aligned}E^{(r)}_{1/q}(x) &\equiv \frac{\mathrm{d}^r}{\mathrm{d}x^r}E_{1/q}(x) \\ &= \sum q^{1/2n(n-1)}\frac{n(n-1)\ldots(n-r+1)}{[n]_J!}x^{n-r}\end{aligned}$$

we find the asymptotic formula for the zeros ($r\geqslant 1$; $n=1,2,\ldots$)

$$x_n^{(r)}=-\frac{q^{-(n+r-1)}}{1-q}\left(\frac{n}{n+1}\right)$$

which can be improved by solving ($p=q^{1/4}$)

$$r!+\sum_{m=1}^{2n-1}p^{2m(m-2n+1)}(m+r)(m+r-1)\ldots(m+1)y^m=0$$

where the improved

$$x_n^{(r)}=-\frac{q^{-(n+r-1)}}{1-q}y_n^{(r)}.$$

Similarly, for the rth indefinite integral

$$E_{1/q}^{(-r)}(x) \equiv \sum_{n=0}^{\infty} \frac{q^{n(n-1)/2}}{(n+r)(n+r-1)\ldots(n+1)} \frac{x^{n+r}}{[n]_J!}$$

$$x_n^{(-r)} = \frac{q^{-(n-1)}}{1-q} y_n^{(-r)} \qquad y_n^{(-r)} \approx -\frac{n+r}{n}$$

$$\frac{1}{r!} + \sum_{m=1}^{2n-1} \frac{p^{2m(m-2n+1)}}{(m+r)(m+r-1)\ldots(m+1)} y^m = 0.$$

Lastly, as in section 5, it is straightforward to directly show for $q > 1$ that the following entire functions are also order zero: $E_q(z)$, $E_q^{(r)}(z)$, $E_q^{(-r)}(z)$, $\mathrm{Cos}_q(z)$ and $\mathrm{Sin}_q(z)$.

Appendix 2. Auxiliary q-boson operators $\tilde{a}_k$, $\tilde{a}_k^+$

Auxiliary q-boson operators were introduced in [7]. For k fixed, we set $\bar{j} \equiv j+k$ and require

$$\tilde{a}_k|\bar{j}\rangle \equiv \begin{cases} [j]^{1/2}|\bar{j}-1\rangle & \text{if } \bar{j} > k \\ \text{zero} & \text{if } \bar{j} \leqslant k \end{cases}$$

and

$$\tilde{a}_k^+|\bar{j}\rangle \equiv [j+1]^{1/2}|\bar{j}+1\rangle \qquad \text{if } \bar{j} \geqslant k.$$

So $\tilde{a}_k|k\rangle = 0$. Then in the $|n\rangle_q$ basis, on the subspace spanned by $|k+j\rangle, j \geqslant 0$,

$$\tilde{a}_k\tilde{a}_k^+ = [\tilde{N}_k + 1]$$

$$\tilde{a}_k^+\tilde{a}_k = [\tilde{N}_k]$$

where $\tilde{N}_k|j+k\rangle = j|j+k\rangle$. Also, $[\tilde{N}_k, \tilde{a}_k^+] = \tilde{a}_k^+$, $[\tilde{N}_k, \tilde{a}_k] = -\tilde{a}_k$. Thus, for each distinct k, $\tilde{a}_k$ and $\tilde{a}_k^+$ are defined on an infinite-dimensional subspace $|k+j\rangle, j \geqslant 0$, and satisfy a quantum algebra

$$\tilde{a}_k\tilde{a}_k^+ - q^{\pm 1/2}\tilde{a}_k^+\tilde{a}_K = q^{\mp \tilde{N}_k/2}$$

on this subspace.

Appendix 3. Other results about $e_q(z)$

Contributions to $e_q(x)$ and $e_q'(x)$ from neglected terms

For $e_q(x)$, the contributions from the neglected terms at the asymptotic zero values, $x = \tilde{\mu}_n^e$, can be systematically evaluated. These corrections arise from the '$\{\} \to 1$' approximation to $[n]!$ in (14a) and from the neglected $r \geqslant 2n$ terms in (17b):

$$e_q(\tilde{\mu}_1) = q^{1/2} - q + O(q^2)$$

$$e_q(\tilde{\mu}_2) = q^{3/2} + O(q^2)$$

$$e_q(\tilde{\mu}_n) = -q + O(q^{3/2}) \qquad n \geqslant 3.$$

Similarly, for the first derivative $e_q'(x)$, we find

$$e_q'(\tilde{\tau}_1)=3q^{1/2}y^2+O(q^{3/2})$$
$$e_q'(\tilde{\tau}_2)=5qy^4+O(q^{3/2})$$
$$e_q'(\tilde{\tau}_3)=7q^{3/2}y^6+O(q^2)$$
$$e_q'(\tilde{\tau}_4)=q^2y^6(9y^2+8y)+O(q^{5/2})$$
$$e_q'(\tilde{\tau}_n)=2nq^2y^{2n-1}+O(q^{5/2}) \qquad n\geqslant 5$$

where $y_n\approx -n/(n+1)$ is the solution to the associated asymptotic polynomial (20).

Properties of the approximate series $e_q^{\mathrm{A}}(x)$

The approximate series $e_q^{\mathrm{A}}(x)$, given in (15), has been introduced as a useful approximation to $e_q(x)$ for $q\ll 1$. As $q\to 0$, both e_q and $e_q^{\mathrm{A}}\to z+1$, *but* as $q\to 1$, $e_q^{\mathrm{A}}\to 1$ and not to the usual $\exp(z)$. Nevertheless, we do find numerically that the exact zeros of the approximate series $e_q^{\mathrm{A}}(x)$ also collide in pairs as q increases above $q_{\mathrm{A}1}^*\approx 0.095$ in a similar manner to what occurs for the q-exponential function itself, $e_q(x)$. For comparison with the (q^*, x^*) values for $e_q(x)$ which are listed in table 2, for $e_q^{\mathrm{A}}(x)$ we find the first five collision points are $(q_{\mathrm{A}1}^*, x_{\mathrm{A}1}^*)=(0.0956, -2.566)$, $(0.2677, -8.263)$, $(0.3977, -14.73)$, $(0.4917, -21.49)$ and $(0.5614, -28.41)$. So the collisions occur at somewhat smaller q^* and x^* values for $e_q^{\mathrm{A}}(x)$ than for $e_q(x)$.

For $q\ll 1$, in the text following (15), the geometric mean $|\bar{x}|=p^{1-2r}(1-q)^{-1}$ of the interval associated with the term '$c_r\bar{x}^r$' in the $e_q^{\mathrm{A}}(x)$ series is introduced. Note that at the geometric mean

$$c_{r-n}|\bar{x}|^{r-n}=p^{-r^2+n^2}$$

gives the value of the other terms of the series (for n negative and positive). Thus, $c_r\bar{x}^r$ dominates the sum in magnitude for $e_q^{\mathrm{A}}(x)$ when

$$|c_r\bar{x}^r|>1+c_1|\bar{x}|+\ldots+c_{r-1}|\bar{x}|^{r-1}+c_{r+1}|\bar{x}|^{r+1}+\ldots$$

or

$$p^{-r^2}>2\{p^{-r^2+1}+p^{-r^2+4}+p^{-r^2+9}+\ldots\}$$

or

$$1>2\{p+p^4+p^9+\ldots+p^{m^2}+\ldots\}.$$

This last inequality holds when $p<0.455\,933\,17\ldots$, $q<0.043\,212\,024\ldots$. Note that in the p^{-r^2} and following other inequality the expressions only go back to $c_0=1$, but go from c_{r+1} on to infinity. So for $q<0.0432$, the $c_r\bar{x}^r$ term does, indeed, dominate the sum in magnitude for the $e_q^{\mathrm{A}}(x)$ series.

References

[1] Exton H 1981 *Proc. Kon. Nederl. Akad. Wetensch.* A **84** 165–71
[2] Exton H 1983 *q-Hypergeometric Functions and Applications* (New York: Ellis Horwood)
[3] MacFarlane A J 1989 *J. Phys. A: Math. Gen.* **22** 4581–8
Biedenharm L C 1989 *J. Phys. A: Math. Gen.* **22** L873–8

[4] Sun C P and Fu H C 1989 *J. Phys. A: Math. Gen.* **22** L983
Chaichian M and Kulish P 1990 *Phys. Lett.* **234B** 72
Kulish P and Damashinsky E 1990 *J. Phys. A: Math. Gen.* **23** L415

[5] Gray R W and Nelson C A 1990 *J. Phys. A: Math. Gen.* **23** L945–50

[6] Chiu S-H, Gray R W and Nelson C A 1992 *Phys. Lett.* **164A** 237

[7] Nelson C A 1992 Novel implications of the q-analogue coherent states SUNY-BING 9/7/92 (to appear in *Symmetrics in Science VI Preprint* (proceedings of a symp at Bregenz, Austria, 1992) ed B Gruber)

[8] Bracken A J, McAnally D S, Zhang R B, and Gould M D 1991 *J. Phys. A: Math. Gen.* **24** 1379

[9] Jurco B 1991 *Lett. Math. Phys.* **21** 51

[10] Exton H 1979 *Proc. R. Soc. London* A **369** 115–36

[11] Jackson F H 1910 *Q. J. Pure Appl. Math.* **41** 193–203

[12] Hille E 1962 *Analytic Function Theory* vol 2 (Boston: Ginn)
Titchmarsh E C 1950 *Theory of Functions* (London: Oxford University Press)
Markushevich A I 1965 *Theory of Functions of a Complex Variable* vol 2 (Engelwood Cliffs, NJ: Prentice-Hall)

[13] Polychronakos A 1990 *Mod. Phys. Lett.* A **5** 2325
Zachos C 1992 *Contemp. Math.* **134** 351
Vokos S and Zachos C 1994 *Mod. Phys. Lett.* A**9** 1

[14] Arik M and Coon D D 1976 *J. Math. Phys.* **17** 524–7

[15] Jackson F H 1904 *Proc. Edin. Math. Soc.* **22** 28–39